CLINICAL RESEARCH ARTICLE

Kawasaki disease OX40–OX40L axis acts as an upstream regulator of NFAT signaling pathway

Yu-Wen Lv[1], Ye Chen[1], Hai-Tao Lv[1], Xuan Li[1], Yun-Jia Tang[1], Wei-Guo Qian[1], Qiu-Qin Xu[1], Ling Sun[1], Guang-Hui Qian[2] and Yue-Yue Ding[1]

BACKGROUND: We investigated a costimulatory molecule OX40–OX40L acting as an upstream regulator to regulate the nuclear factor of activated T cell (NFAT) in the acute phase of Kawasaki disease (KD).
METHODS: One hundred and one samples were collected and divided into six groups: coronary artery lesion (KD-CAL) before intravenous immunoglobulin (IVIG), KD-CAL after IVIG, KD without CAL (KD-nCAL) before IVIG, KD-nCAL after IVIG, fever of unknown (Fou), and Healthy. In vitro OX40-stimulating and OX40L-inhibiting tests were conducted in Healthy and KD groups, respectively. Both the messenger RNA (mRNA) and protein expression levels of OX40, OX40L, NFAT1, and NFAT2 were investigated using quantitative reverse transcription PCR and immunoblotting assay, respectively.
RESULTS: The mRNA and protein expression levels of NFAT1, NFAT2, OX40, and OX40L were significantly increased in KD-CAL and KD-nCAL groups before IVIG compared with Fou and Healthy groups and decreased after IVIG. A positive correlation was found between them in KD. In vitro OX40-stimulating test demonstrated the significantly increased mRNA and protein expression levels of NFAT1 and NFAT2 in the peripheral blood mononuclear cells of the Healthy group. Meanwhile, OX40L-inhibiting test showed significantly decreased expression levels of NFAT1 and NFAT2 in the KD group.
CONCLUSION: OX40–OX40L acts as an upstream regulator in the NFAT signaling pathway involved in KD.

INTRODUCTION

Kawasaki disease (KD) is a systemic vascular disease preferentially occurring in infants and children.[1,2] It is characterized by the development of coronary artery aneurysms (CAAs), which may result in fatal thrombosis and sudden cardiac failure. Clinical manifestations of KD include prolonged fever (1–2 weeks, mean 10–11 days), conjunctival infection, oral lesions, polymorphous skin rashes, extremity changes, and cervical lymphadenopathy, all of which comprise the diagnostic criteria.[3] KD is a kind of excessive inflammatory activation of autoimmune disease, but the mechanisms resulting in immune dysfunction remain unknown.[4–6]

The activation of the immune system and the cascade of inflammatory factors are considered as important features of KD. A large number of T cells, mononuclear cells, macrophages, and plasma cells, with a smaller number of neutrophils, are observed in various organ tissues of fatal cases in acute KD. Our published study[7] and previous literatures[8–12] implied that nuclear factor of activated T cell (NFAT) signaling pathway is involved in the immune damage process of KD. NFAT is a family of transcription factors identified in activated T cells.[13] Both NFAT1 and NFAT2 play major roles in this progress, but the upstream links are not clear. OX40 and its ligand OX40L are less well-explored members of the tumor necrosis factor receptor family. They are a pair of important costimulatory molecules in the process of immune response. Studies have shown that OX40 and OX40L play important roles in inflammatory diseases, autoimmune diseases,

tumor, and immune transplant.[14,15] Meanwhile, OX40–OX40L axis functioning as important costimulatory molecules in the immune response can activate NFAT signal channels and promote the expression of inflammatory molecules involved in the development of atherosclerosis.[16,17]

Considering the essential roles of OX40, OX40L, and NFAT signaling pathway in immune response, we speculated that OX40 and OX40L are likely to be involved in the immune damage process of KD through regulating NFAT. At present, there are no reports studying the relationship between OX40, OX40L, and KD. In this work, we examined the expression level of OX40, OX40L, NFAT1, and NFAT2 in KD and analyzed the correlation between OX40, OX40L, and NFAT1 and NFAT2 to validate the possibility of OX40–OX40L–NFAT signaling pathways in KD immune injury. After stimulating and inhibiting the OX40–OX40L interactions in the cultured peripheral blood mononuclear cells (PBMCs) from Healthy and KD groups, respectively, we examined the expression levels of NFAT1, NFAT2 mRNA, and protein to validate the regulation of OX40–OX40L–NFAT axis involved in Kawasaki disease.

METHODS

In vivo study on exploring the expression of OX40, OX40L, NFAT1, and NFAT2 in KD
Groups. (1) KD group: 55 KD children, including 42 males and 13 females, 3 months–5 years and 3 months old (2.6 ± 0.5 years on

[1]Cardiology Department, Children's Hospital of Soochow University, 215025 Suzhou, Jiangsu Province, China and [2]Institute of Pediatric Research, Children's Hospital of Soochow University, 215025 Suzhou, Jiangsu Province, China
Correspondence: Guang-Hui Qian (ghqian@suda.edu.cn) or Yue-Yue Ding (dyyqd79@hotmail.com)
These authors contributed equally: Yu-Wen Lv, Ye Chen

836

average), were all in-patients in Children's Hospital of Soochow University. They conformed to the diagnostic criteria revised by AHA Kawasaki Disease Guideline.[3] Based on echocardiography examination results, the KD groups were divided into two subgroups, 12 cases in coronary artery lesion group (KD-CAL) and 43 cases in non-CAL group (KD-nCAL). According to whether they were injected with intravenous immunoglobulin (IVIG), the KD-CAL and KD-nCAL subgroups were divided into two groups, respectively, named KD-CAL before, KD-CAL after, and KD-nCAL before and KD-nCAL after.[2] Fever of the unknown control group (Fou): 23 cases of inpatients with acute fever, having matched sex and age as in the KD group, were proven to have respiratory infection excluding out other connective tissue diseases, such as juvenile rheumatoid arthritis, and tuberous polyarteritis as supplemental condition.[3] Healthy control group (Healthy): 23 children with matched sex and age, visiting the hospital for physical examination. The Children's Hospital of Soochow University ethics committee approved this study. Methods were carried out in accordance with the approved guidelines. An informed written consent was obtained from the parents of each patient.

Treatment protocol of KD. Standard treatment given for KD was as follows: patients were treated with IVIG (2 g/kg) in a single infusion, together with high-dose aspirin administered at 30–50 mg/kg/day if they were presented within the first 5–10 days of illness. Repeat treatment with IVIG was considered if patients had persistent fever without other explanations, 48 h after initial therapy. High-dose aspirin was continued until ≥48–72 h after fever cessation. Then, low-dose aspirin (3–5 mg/kg/day) was initiated and maintained until the patient showed no evidence of coronary changes for 6–8 weeks after the onset of illness. For children who developed coronary abnormalities, aspirin was continued indefinitely. Steroid treatment was restricted to children in whom ≥2 infusions of IVIG had been ineffective in alleviating fever and acute inflammation. The steroid regimen consisted of an intravenous pulse of methylprednisolone at 30 mg/kg for 2–3 h, administered once daily for 1–3 days.

Extracting and processing of PBMCs. From each enrolled child, 2 mL of venous blood was taken and put into anticoagulation tubes with ethylene diamine tetraacetic acid (EDTA) for blending and centrifugalizing at 1500 r/min under 4 °C for 5 min. In order to isolate the white blood cells (WBCs), the ACK Lysis Buffer was added to cell sedimentation in the ratio of 1:6–10, centrifuged at 1500 r/min under 4 °C for 5 min again, and then washed with phosphate-buffered saline solution twice. Further, to obtain PBMCs, Ficoll-Paque (Amersham Pharmacia Biotech, Herts, UK), the reagent of density gradient centrifugation, was added into the EDTA-anticoagulated whole-blood samples. The isolated PBMCs were used in the later stimulation and inhibition experiments in vitro. Then, the isolated WBCs and PBMCs were preserved at −80 °C for real-time PCR and Western blot, in order to measure the mRNA and protein expression of OX40, OX40L, NFAT1, and NFAT2.

In vitro study on exploring the regulation roles of OX40–OX40L axis on NFAT signaling pathway
Cell culture. The 24-well plates were coated overnight with anti-CD3 antibody (10 mg/mL; Bo Hui biotechnology company, Wuxi, Jiangsu) at 4 °C. Unbound antibody was washed away before adding cells. The PBMCs from Healthy and KD children were separated with Ficoll-Paque, and the cellular suspensions were cultured in 24-well plates at an initial density of 2×10^6 cells per well, respectively, all having three vice holes. Cells were maintained in 5% CO_2 at 37 °C.

Stimulating test. According to our pretest of the difference of time and concentration gradient, we found the best stimulating time and concentration, respectively.[18] Anti-OX40 monoclonal antibody (OX86, Santa Cruz), 40 µg/mL was used to stimulate OX40–OX40L axis in PBMCs from normal samples for 48 h, and the PBMCs of normal samples before stimulation were used as the control group. The mRNA and protein expression levels of NFAT1 and NFAT2 in PBMCs were measured by quantitative reverse transcription PCR (RT-qPCR) and Western blot analysis, respectively.

Inhibiting test. Anti-OX40L monoclonal antibody (RMl35L, Santa Cruz), 20 µg/mL was used to inhibit OX40–OX40L axis in the PBMCs of KD group for 24 h. The PBMCs of the KD group before inhibition were used as the control group. The mRNA and protein expression levels of NFAT1 and NFAT2 in PBMCs were measured by RT-qPCR and Western blot analysis, respectively. According to the difference of time and concentration gradient, we found the best inhibiting time and concentration, respectively.

Real-time PCR
Total RNA was prepared by RNA-TRIZOL extraction (Gibco). The RNA was quantified and reverse-transcribed according to the manufacturer's protocol. Quantitative gene expression analysis was performed on an ABI 7500 (America) using Ascent software for Multiskan. PCR thermal cycling conditions were 95 °C for 10 min, and 40 cycles of 95 °C for 10 s and 60 °C for 1 min. Transcript levels of target genes were calculated according to the $2^{-\Delta\Delta CT}$ Method. Sequences of primers were given in Table 1.

Western blot
Cells were lysed in 50 mmol/L Tris-HCl/150 mmol/L NaCl (pH 7.5) ice-cold buffer containing 1% Nonidet P40, 0.5% sodium deoxycholate, 100 mmol/L NaF, 2 mmol/L Na_3VO_4, 10 mmol/L phenylmethylsulfonyl fluoride, 500 µmol/L 4-(2-aminoethyl)-benzenesulfonyl fluoride, 150 nmol/L aprotinin, and 1 µmol/L leupeptin. Protein concentration was determined with the use of BCA Protein Assay Kit. Proteins (30 µg) were electrophoresed in 12% sodium dodecyl sulfate-polyacrylamide gel and transferred to nitrocellulose membranes. Bands were visualized by reaction with specific antibodies directed against NFAT1, NFAT2, OX40, and OX40L. In brief, membranes were blocked in 5% bovine serum albumin for 2 h at room temperature and probed with anti-NFAT1, NFAT2, OX40, and OX40L antibodies (Santa Cruz Biotechnology, Inc.) for 1 h at room temperature, respectively. Given that the molecular weight of NFAT1 and glyceraldehyde 3-phosphate dehydrogenase (GAPDH) protein are close to each other, three sodium dodecyl sulfate-polyacrylamide gel electrophoresis experiments were conducted to detect the expression level of each protein with a specific antibody, respectively. After secondary incubation in horseradish peroxidase–anti-mouse IgG antibody (Santa Cruz Biotechnology, Inc.), the immunocomplexes were visualized with an enhanced chemiluminescence detection kit according to the manufacturer's instructions and quantified by densitometry. As a control, the expression of GAPDH was analyzed in parallel. For some cases, due to a small amount of proteins isolated from PBMCs of KD patients, 34 KD-nCAL protein samples were mixed and therefore grouped in 17 samples. While the remaining 21 protein samples of KD patients were extracted directly. We configured the normalization to the total protein visualized with GAPDH. This practice ensured correction for the amount of total protein on the membrane in the case of errors or incomplete transfers. The ratio of integrated optical density of target protein expression to that of GAPDH expression was calculated to represent the relative expression amount of target protein lysed from PBMCs.

Statistical analysis
Data were expressed as mean ± standard deviation (SD) and analyzed by SPSS17.0 software. For comparisons between two variables, the unpaired Student's *T* test was used. Comparisons

Kawasaki disease OX40–OX40L axis acts as an upstream regulator...
Y.-W. Lv et al.

837

Table 1. Sequence of primers used in real-time RT-PCR

Gene	Forward primer (5′ → 3′)	Reverse primer (5′ → 3′)
NFAT1	GGGCTTCTACAACGACGTGGTC	ACAGATTGCGTCCGAGCTATTGC
NFAT2	GATTCTACGATTGCAGCGCAGTG	AACCGCCTTGCAGAAGTTGTC
OX40L	TCTACAGCTTTGGCGAGTC	CAAATGTTGACCACGCTGCTATC
OX40	GGGCTTCTACAACGACGTGGTC	ACAGATTGCGTCCGAGCTATTGC

RT-PCR reverse transcription PCR

Table 2. The clinical features of all patients

Group	KD		Fou	Healthy
	CAL	nCAL		
Age				
3–24 months	9	35	17	19
>24 months	3	8	6	4
Sex				
Male	8	33	15	15
Female	4	10	8	8
IVIG				
IVIG nonresponders	2	3		

KD Kawasaki disease, CAL coronary artery lesion, nCAL without coronary artery lesion, IVIG intravenous immunoglobulin, Fou fever of unknown
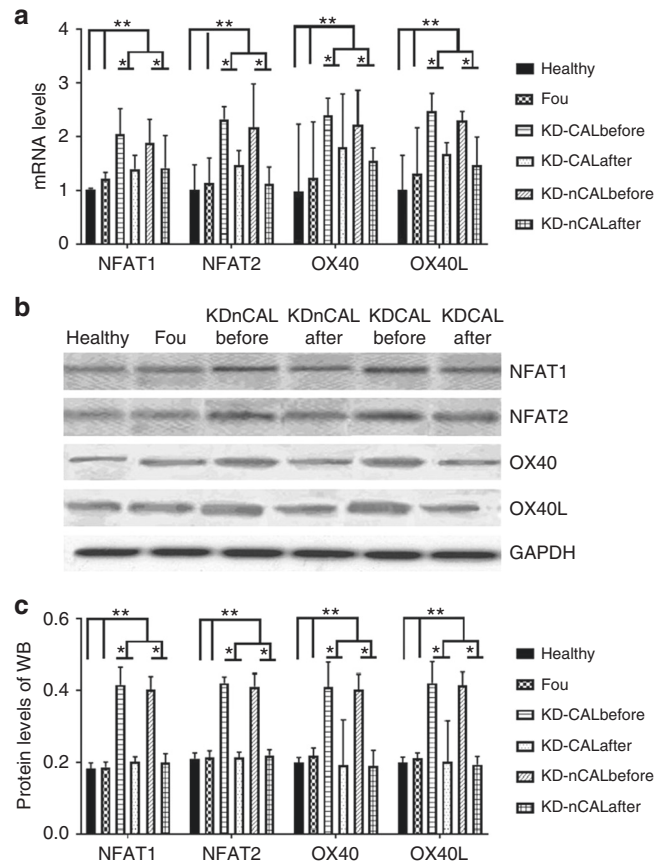

Fig. 1 The messenger RNA (mRNA) expression of nuclear factor of activated T cell 1 (NFAT1), NFAT2, OX40, OX40L of quantitative reverse transcription PCR (RT-qPCR) analysis, and the relative protein expression levels of Western blot analysis in the groups of Healthy, fever of unknown (Fou), Kawasaki disease (KD) without coronary artery lesion group (KD-nCAL), and coronary artery lesion group (KD-CAL) before and after treatment. **a** The mRNA expression levels in each group. **b** Western blot analysis of all groups, each band represents the protein from the lysed peripheral blood mononuclear cells (PBMCs). **c** The protein expression levels of all groups. (*$p < 0.05$ indicates significant differences in the KD-nCAL and KD-CAL groups before and after intravenous immunoglobulin (IVIG) treatment; **$p < 0.05$ indicates significant differences among the groups of KD, Heathy, and Fou)

among more than two groups involved one-way analysis of variance followed by post hoc least significant difference test. Correspondence analysis was used by Pearson correlation in SPSS. A two-tailed $p < 0.05$ was considered statistically significant.

RESULTS
In vivo study on exploring the expression levels of OX40, OX40L, NFAT1, and NFAT2 molecules in the KD group
Clinical features of KD. There were no significant difference in gender and age among KD, Healthy, and Fou groups ($p > 0.05$). Out of 55 KD patients, excluding 5 people who did not respond to IVIG and were subsequently given an intravenous pulse of methylprednisolone, 12 with coronary aneurysm were given oral low-dose aspirin for 3–36 months and the remaining patients were given standard treatment (Table 2).

The expression levels of OX40, OX40L, NFAT1, and NFAT2 in KD. The mRNA expression levels of NFAT1, NFAT2, OX40, and OX40L in the PBMCs of KD patients with or without CAL increased significantly compared with the Healthy or Fou groups ($p < 0.05$), and they were not statistically higher in the subgroups of CALs than nCALs before IVIG treatment ($p > 0.05$). The results also showed that the mRNA expression levels of the above four molecules decreased remarkably in the KD patients, whether complicated with CAL or not after IVIG treatment ($p < 0.05$).

Consistently, the protein expression levels of NFAT1, NFAT2, OX40, and OX40L also showed similar expression tendency among the KD, Healthy, and Fou groups. Notably, the increased protein expression levels of NFAT1, NFAT2, OX40, and OX40L in KD patients with or without CAL declined remarkably after IVIG treatment ($p < 0.05$) (Fig. 1).

The correlation analysis of OX40, OX40L, and NFAT1 and NFAT2 in KD. A significant positive correlation was demonstrated for the relative protein expression levels of OX40, OX40L, and NFAT1 and

NFAT2 lysed from PBMC of KD patients before IVIG treatment ($p < 0.05$) (Table 3, Fig. 2). There was no significant correlation between Healthy and Fou groups (all $p > 0.05$).

In vitro study on exploring the regulation roles of OX40–OX40L axis on NFAT signaling pathway
Importantly, both the mRNA and protein expression levels of NFAT1 and NFAT2 in the PBMCs isolated from the Healthy group

increased significantly on stimulation with anti-OX40 monclonal antibody (mAb) in vitro ($p < 0.05$). Meanwhile, the mRNA and protein expression levels of NFAT1 and NFAT2 in the PBMCs isolated from the KD group were suppressed remarkably on inhibition with anti-OX40L mAb in vitro ($p < 0.05$) (Fig. 3).

DISCUSSION

KD is now recognized as the leading cause of acquired heart disease in children in the developed and developing countries of Asia. The underlying etiology and mechanisms leading to vessel injuries that are the hallmarks of KD remain largely unknown.

Previous studies suggested that NFAT signaling pathway is involved in the pathological process of KD.[18] NFAT was critical for the expression of a number of immune cytokines, including IL-1, IL-2, IL-4, IL-5, and IL-13. The combined effect of these factors may

lead to the vascular damage and formation of CALs in KD. Onouchi reported that inositol-trisphosphate 3-kinase C (ITPKC) acted as a negative regulator of T-cell activation via the Ca^{2+}/NFAT signaling pathway in KD.[19] Further research confirmed that a novel ITPKC-interacting protein, namely PPP3CC, could inhibit phosphorylation of ITPKC and consequently prevent ITPKC from ubiquitin-mediated protein degradation.[20] Meanwhile, the ORAI1 gene, encoding for a calcium channel, was found to influence the KD susceptibility.[21] Both the ITPKC and ORAI1 gene involved in the regulation of calcium flux in the cell and induced NACHT, LRR, and PYD domains-containing protein 3 (NLRP3) inflammasome activation and secretion of interleukin-1β (IL-1β) and IL-1α. A few studies had confirmed that IL-1β was a master mediator of innate immunity and inflammation as a key cytokine of IVIG- treating CALs. IL-1β was transcribed as an inactive precursor that required assembly of the NLRP3 inflammasome to activate caspase-1, the enzyme that cleaved pro-IL-1β to release the biologically active form of the cytokine.[22–24] Previous analysis revealed the critical role of ITPKC in mediating NLRP3 inflammasome activation, and identified that regulation of calcium mobilization is fundamental to the underlying immunobiology in KD.[25] As a result, we speculated that Ca^{2+}/NFAT and Ca^{2+}/NLRP3/IL-1β signaling pathways could function synergistically to a wide range of roles in the pathological process of KD.

In this study, we found that the mRNA and relative protein expression levels of NFAT1 and NFAT2 in the WBC samples of the KD group were significantly increased than those of the control groups. The result indicated that NFAT involved in the acute phase of KD acting as a potential major role on activated T cell. However, there was no adequate evidence to verify the association between

Table 3. The correlation of expression level between OX40, OX40L, and NFAT1 and NFAT2 in the KD group before IVIG treatment

KD group	OX40		OX40L	
	r	P value	r	P value
NFAT1	0.438	<0.01	0.336	<0.01
NFAT2	0.596	<0.01	0.586	<0.01

IVIG intravenous immunoglobulin, *KD* Kawasaki disease, *NFAT* nuclear factor of activated T cell
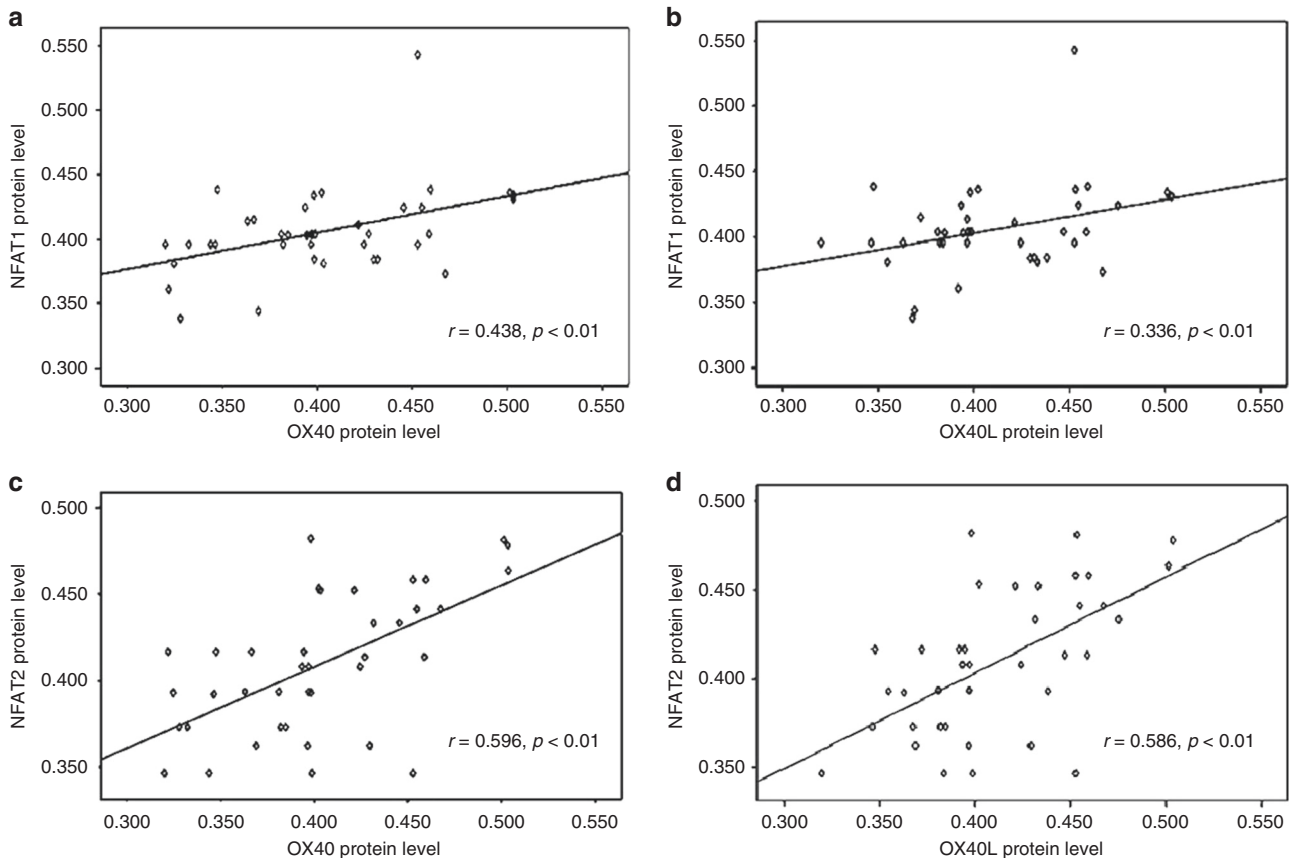

Fig. 2 The correlation analysis of the protein expression levels of OX40, OX40L, and nuclear factor of activated T cell 1 (NFAT1) and NFAT2 in Kawasaki disease (KD) before intravenous immunoglobulin (IVIG) treatment. **a** The correlation between NFAT1 and OX40. **b** The correlation between NFAT1 and OX40L. **c** The correlation between NFAT2 and OX40. **d** The correlation between NFAT2 and OX40L.
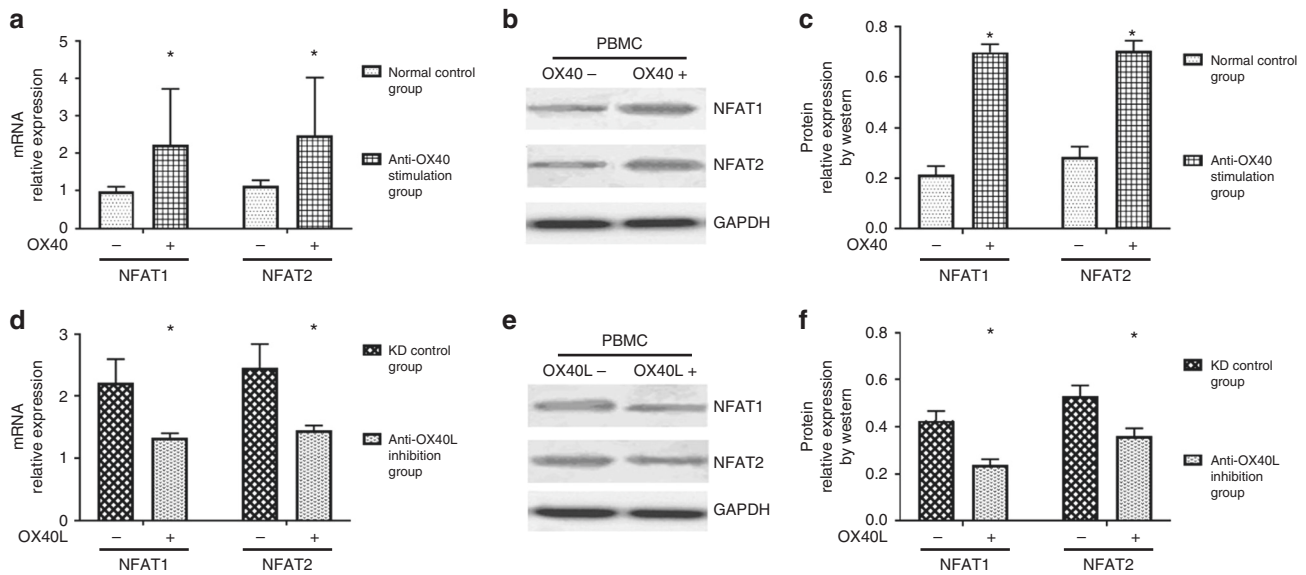
Kawasaki disease OX40–OX40L axis acts as an upstream regulator...
Y.-W. Lv et al.

839

Fig. 3 The expression levels of nuclear factor of activated T cell 1 (NFATI), NFAT2 messenger RNA (mRNA) of quantitative reverse transcription PCR (RT-qPCR) analysis, and protein expression levels of Western blot analysis following stimulation or inhibition by anti-OX40/anti-OX40L antibody. **a** The expression levels of NFATI and NFAT2 mRNA followingstimulation by anti-OX40 antibody. **b** Western blot analysis of two groups stimulated or not by anti-OX40 antibody to normal peripheral blood mononuclear cells (PBMCs). **c** The protein expression levels of NFATI and NFAT2 following stimulationd by anti-OX40 antibody. **d** The expression levels of NFATI and NFAT2 mRNA following inhibition by anti-OX40L antibody. **e** Western blot analysis of two groups inhibited or not by anti-OX40L antibody in PBMCs of Kawasaki disease. **f** The protein expression levels of NFATI and NFAT2 following inhibition by anti-OX40L antibody (*$p < 0.05$ indicates that the groups have significant differences with the groups following stimulation/inhibition)

NFAT1, NFAT2, and the coronary lesions of KD. The regulatory mechanism still remained unknown.

Furthermore, strong correlations were noted between the protein expression levels of OX40–OX40L and NFAT in the acute phase of KD, which suggested a potential positively regulating mechanism between the signaling pathways of OX40–OX40L and NFAT in KD. OX40–OX40L signaling pathway has been shown to play certain curative effect in many animal models (experimental autoimmune encephalomyelitis, rheumatoid arthritis, graft-vs.-host disease, inflammatory bowel disease, and atherosclerosis).[26–32] Blocking OX40–OX40L axis may be a new target for the management of immune injury of KD.

OX40–OX40L signal may promote hyperplasia of CD4^{+} T-cell clone, strengthen the function of cell effect, induce the generation of memory T cells, and extend the survival time of T cell, which could interact with the NFAT signaling pathway.[33,34] Jin-chuan et al.[35] suggested that OX40–OX40L interaction regulates the expression of NFATc1 in the apolipoprotein E-deficient mice with atherosclerosis. A clinical study confirmed the correlation between OX40–OX40L and NFAT in the PBMCs of KD patients. But in order to validate the regulation relationships between OX40–OX40L axis and NFAT signaling pathway from the mechanism, more evidence and approaches would be needed. Further studies, for example, loss- and gain-of-function tests, should be improved in the follow-up experiments.

In this work, the gene and protein expression values of OX40 and OX40L in the KD group were significantly higher than those in the control groups, which indicated that OX40 and OX40L participated in the immune activation process in the acute phase of KD. Prior studies reported that OX40–OX40L axis may increase the inflow intracellular Ca^{2+}, accelerate the shift of NFAT in the nuclei, and further mediated amplification, split, and survival of T cells.[36,37] Clinically, we found the correlation between OX40–OX40L and NFAT pathway. In order to validate the regulatory relationship between OX40–OX40L axis and NFAT, further in vitro experiments were conducted. When stimulating the OX40–OX40L axis, the expression of NFAT1, NFAT2 mRNA, and protein was significantly higher than those in the control group. On the contrary, when inhibiting the OX40–OX40L axis, the expression of NFAT1, NFAT2 mRNA, and protein remarkably decreased. The in vitro experiment confirmed the interactive association between OX40–OX40L and NFAT. As a result, OX40–OX40L axis could serve as an upstream regulatory signal in the pathogenesis of KD functioning as by activating the NFAT signaling pathway, it may involve in the immune damage process of KD.

CONCLUSION
The expression of NFAT1, NFAT2, OX40, and OX40L was highly synchronized in the acute phase of KD. By stimulating and inhibiting the OX40–OX40L axis, the expression of NFAT1 and NFAT2 was varied. Blocking the OX40–OX40L signal axis may be a new target for the management of immune injury in KD.

AUTHOR CONTRIBUTIONS
Y.-W.L. carried out the studies and wrote the paper and Y.C. participated in its design and wrote the paper. H.-T.L. helped to design the manuscript and wrote the paper. X.L., Y.-J.T., W.-G.Q., Q.-Q.X., and L.S. participated in the collection of clinical cases. G.-H.Q., as the co-corresponding author, participated in the experimental process.

Kawasaki disease OX40–OX40L axis acts as an upstream regulator...
Y.-W. Lv et al.

840

Y.-Y.D., as the first corresponding author, participated in the design of the whole study and wrote the manuscript. All authors read and approved the final manuscript.

ADDITIONAL INFORMATION

REFERENCES

1. Saguil, A., Fargo, M. & Grogan, S. Diagnosis and management of kawasaki disease. *Am. Fam. Physician* **91**, 365–371 (2015).
2. Dietz, S. M. et al. Dissecting Kawasaki disease: a state-of-the-art review. *Eur. J. Pediatr.* **176**, 995–1009 (2017).
3. McCrindle, B. W. et al. American Heart Association Rheumatic Fever, Endocarditis, and Kawasaki Disease Committee of the Council on Cardiovascular Disease in the Young; Council on Cardiovascular and Stroke Nursing; Council on Cardiovascular Surgery and Anesthesia; and Council on Epidemiology and Prevention. Diagnosis, Treatment, and Long-Term Management of Kawasaki Disease: A Scientific Statement for Health Professionals From the American Heart Association. *Circulation* **135**, e927–e999 (2017).
4. Pilania, R. K., Bhattarai, D. & Singh, S. Controversies in diagnosis and management of Kawasaki Disease. *World J. Clin. Pediatr.* **7**, 27–35 (2018).
5. Newburger, J. W., Takahashi, M. & Burns, J. C. Kawasaki disease. *J. Am. Coll. Cardiol.* **67**, 1738–1749 (2016).
6. Kuo, H. C. et al. Wireless optical monitoring system dentifies limb induration characteristics in Kawasaki disease. J *Allergy Clin. Immunol.* pii: S0091-6749(18) 30631-6 (2018).
7. Lv, Y. W. et al. Understanding the pathogenesis of Kawasaki disease by network and pathway analysis. *Comput. Math. Methods Med.* **2013**, 989307 (2013).
8. Kim, K. Y. et al. ITPKC and SLC11A1 gene polymorphisms and gene–gene interactions in Korean patients with Kawasaki disease. *Yonsei. Med. J.* **59**, 119–127 (2018).
9. Khor, C. C. et al. Genome-wide association study identifies FCGR2A as a susceptibility locus for Kawasaki disease. *Nat. Genet.* **43**, 1241–1246 (2011).
10. Onouchi, Y. et al. A genome-wide association study identifies three new risk loci for Kawasaki disease. *Nat. Genet.* **44**, 517–521 (2012).
11. Onouchi, Y. The genetics of Kawasaki disease. *Int J. Rheum. Dis.* **21**, 26–30 (2018).
12. Renauer, P., Coit, P. & Sawalha, A. H. Epigenetics and vasculitis: a comprehensive review. *Clin. Rev. Allergy Immunol.* **50**, 357–366 (2016).
13. Lee, J. U., Kim, L. K. & Choi, J. M. Revisiting the concept of targeting NFAT to control T cell immunity and autoimmune diseases. *Front. Immunol.* **9**, 2747 (2018).
14. Chang, Y. K. et al. Association of BANK1 and TNFSF4 with systemic lupus erythematosus in Hong Kong Chinese. *Genes Immun.* **10**, 414–420 (2009).
15. Nuebling, T. et al. The immune checkpoint modulator OX40 and its ligand OX40L in NK-cell immunosurveillance and acute myeloid leukemia. *Cancer Immunol. Res.***6**,209-221 (2018)
16. Jin-chuan, Y. OX40-OX40L interaction promotes proliferation and activation of lymphocytes via NFATc1 in ApoE-deficient mice. *PLoS ONE* **8**, e60854 (2013).
17. Yan, J., Wang, C., Du, R., Liu, P. & Chen, G. OX40-OX40L ligand interaction may activate phospholipase C signal transduction pathway in human umbilical vein endothelial cells. *Chem. Biol. Interact.* **180**, 460–464 (2009).
18. Wang, W. et al. The roles of Ca^{2+}/NFAT signaling genes in Kawasaki disease: single- and multiple-risk genetic variants. *Sci. Rep.* **6**, 5208 (2014).
19. Onouchi, Y. et al. ITPKC functional polymorphism associated with Kawasaki disease susceptibility and formation of coronary artery aneurysms. *Nat. Genet.* **40**, 35–42 (2008).
20. Li, P. et al. PPP3CC feedback regulates IP3-Ca^{2+} pathway through preventing ITPKC degradation. *Front Biosci. (Landmark Ed.)* **18**, 919–927 (2013).
21. Onouchi, Y. et al. Variations in ORAI1 gene associated with Kawasaki disease. *PLoS ONE* **11**, e0145486 (2016).
22. Burns, J. C. et al. Found in translation: international initiatives pursuing interleukin-1 blockade for treatment of acute Kawasaki disease. *Arthritis Rheumatol.* **69**, 268–276 (2017).
23. Wakita, Daiko et al. The role of IL-1 signaling in a mouse model of Kawasaki disease-associated abdominal aortic aneurysm. *Arterioscler. Thromb. Vasc. Biol.* **36**, 886–897 (2016).
24. Lee, Y. et al. Interleukin-1β is crucial for the induction of coronary artery inflammation in a mouse model of Kawasaki disease. *Circulation* **125**, 1542–1550 (2012).
25. Alphonse, M. P. et al. Response in Kawasaki disease inflammasome activation and treatment inositol-triphosphate 3-kinase C mediates. *J. Immunol.* **197**, 3481–3489 (2016).
26. Adcock, I. M., Caramori, G. & Chung, K. F. New targets for drug development in asthma. *Lancet* **372**, 1073–1087 (2008).
27. Hanania, N. A. Targeting airway inflammation in asthma: current and future therapies. *Chest* **133**, 989–998 (2008).
28. Cavanagh, M. M. & Hussell, T. Is it wise to target the late costimulatory molecule OX40 as a therapeutic target? *Arch. Immunol. Ther. Exp. (Warsz.)* **56**, 291–297 (2008).
29. Fujita et al. Functional characterization of OX40 expressed on human CD8+ T cells. *Immunol. Lett.* **106**, 27–33 (2006).
30. So, T., Lee, S. W. & Croft, M. Immune regulation and control of regulatory T cells by OX40 and 4-1BB. *Cytokine Growth Factor Rev.* **19**, 253–262 (2008).
31. Marschner, A. et al. CpG ODN enhance antigen-specific NKT cell activation via plasmacytoid dendritic cells. *Eur. J. Immunol.* **35**, 2347–2357 (2005).
32. Zaini, J. et al. OX40 ligand expressed by DCs costimulates NKT and CD4+ Th cell antitumor immunity in mice. *J. Clin. Invest.* **117**, 3330–3338 (2007).
33. Croft, M., So, T. & duan, W. The significance of OX40 and OX40L to T-cell biology and immune disease. *Immunol. Rev.* **229**, 173–191 (2009).
34. Beier, K. C., Kallinich, T. & Hamelmann, E. Master switches of T-cell activation and differentiation. *Eur. Respir. J.* **29**, 804–812 (2007).
35. Jin-chuan, Y. et al. Effects of OX40–OX40L interaction on the nuclear factor of activated T cells c1 in ApoE-deficient mice. *Inflammation* **37**, 205–213 (2014).
36. Latza, U. et al. The human OX40 homolog: eDNA structure, expression and chromosomal assignment of the ACT35 antigen. *Eur. J. Immunol.* **24**, 677–683 (1994).
37. Mallett, S., Fossum, S. & Barclay, A. N. Characterization of the MRC OX40 antigen of activated CD4 positive T lymphocytes-a molecule related to nerve growth factor receptor. *EMBO J.* **9**, 1063–1068 (1990).